



Comparing LSNA Calibrations

*Paweł Barmuta, Diogo Ribeiro,
Kuangda Wang, Gustavo Avolio, Mohammad Rajabi,
Arkadiusz Lewandowski, Gian Piero Gibiino,
Jarosław Szatkowski, Dominique Schreurs, Paul Hale,
Kate Remley, and Dylan Williams*

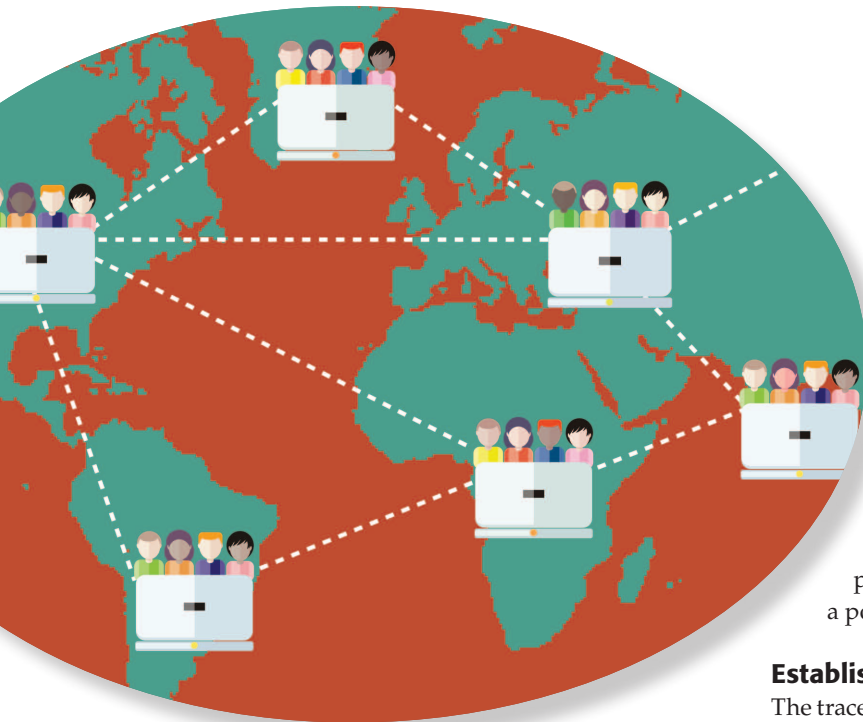


IMAGE LICENSED BY INGRAM PUBLISHING

Large-signal network analyzers (LSNAs) provide direct measurements of the nonlinear behavior of active devices under realistic operating conditions.

Large-signal measurements facilitate the extraction of more accurate transistor and power amplifier models. This is a key factor in the development of better communications systems by use of modern modulation schemes [1].

However, the calibration of LSNAs is very challenging. In addition to a conventional linear scattering-parameter calibration, the calibration of an LSNA requires two extra standards: a phase reference (e.g., a comb generator) and a power meter [1].

Establishing Traceability for Calibration

The traceability (i.e., an unbroken chain of measurements and associated uncertainties to a primary reference [2]) for the linear scattering-parameter

Paweł Barmuta (Pawel.Barmuta@esat.kuleuven.be) is with KU Leuven, Belgium, and Warsaw University of Technology, Poland. Diogo Ribeiro (dribeiro@ua.pt) is with the University of Aveiro, Portugal, and the National Institute of Standards and Technology, Boulder, Colorado, United States. Kuangda Wang (kuangda.wang@polymtl.ca) is with the Ecole Polytechnique de Montreal, Canada. Gustavo Avolio (gustavo.avolio@esat.kuleuven.be), Mohammad Rajabi (Mohammad.Rajabi@esat.kuleuven.be), and Dominique Schreurs (Dominique.Schreurs@kuleuven.be) are with KU Leuven. Arkadiusz Lewandowski (A.Lewandowski@elka.pw.edu.pl) and Jarosław Szatkowski (J.Szatkowski@stud.elka.pw.edu.pl) are with the Warsaw University of Technology. Gian Piero Gibiino (gianpiero.gibiino@esat.kuleuven.be) is with KU Leuven and the University of Bologna, Italy. Paul Hale (paul.hale@nist.gov), Kate Remley (kate.remley@nist.gov), and Dylan Williams (dylan.williams@nist.gov) are with the National Institute of Standards and Technology, Boulder, Colorado.

Digital Object Identifier 10.1109/MMM.2015.2499043
Date of publication: 14 January 2016

In addition to a conventional linear scattering-parameter calibration, the calibration of an LSNA requires two extra standards: a phase reference (e.g., a comb generator) and a power meter.

part of the calibration is achieved with traceable mechanical measurements. However, establishing traceability for the phase references used to calibrate LSNA's to basic physical quantities requires precision waveform measurements [3], [4]. In addition, the nonlinear elements are prone to temperature changes and aging, as they are based on the active components [5], [9]. Moreover, comparing large-signal measurements is not straightforward, as each LSNA presents different impedances to nonlinear test artifacts at the fundamental and harmonics.

Several attempts have been undertaken to develop a special reference device that will provide well characterized and stable nonlinear response [6]–[8]. However, it is difficult to infer how accurately an LSNA will perform measurements from the measurement of a single nonlinear reference device, even if the single reference device has been perfectly characterized and its response does not depend on the impedances that the LSNA presents to it. Identifying the source of errors of the user's calibration, should measurements not agree, is also difficult.

An alternative "calibration-comparison" approach was proposed in [10]. Instead of using a single nonlinear reference device to characterize an LSNA, a complete and traceable calibration kit (consisting of additional scattering-parameter calibration artifacts, phase reference, and power meter) is used to assess the accuracy of a user's working calibration. The procedure outlined in [10] accomplishes this by comparing the calibration coefficients that are based on the user's calibration approach with the calibration coefficients that are based on the traceable calibration kit. With this method, both the calibration algorithms used and the definition of the calibration standards are compared simultaneously.

The LSNA Round-Robin Student Design Competition

Here, we report on the LSNA Round-Robin Student Design Competition held at the IEEE International Microwave Symposium in May of 2015. This competition was the first test of the calibration-comparison method of [10] in a measurement round robin taking place in three measurement laboratories. The round robin was targeted at characterizing the overall accuracy of the measurements performed in each laboratory with the procedures and calibration artifacts available in that laboratory. This includes assessing

the calibration approaches employed in the laboratory, the care with which calibrations are performed in the laboratory, differences in the instrumentation used, and the accuracy of the scattering-parameter, power, and comb generators used in the calibrations. The round robin was also designed to diagnose, to the greatest extent possible, the largest sources of error in the measurements performed in that laboratory from the calibration-comparison results.

To accomplish this, a single nonlinear calibration kit was characterized at the National Institute of Standards and Technology (NIST) and distributed sequentially to the three teams: one in Leuven, Belgium, and Warsaw, Poland (P. Barnuta, M. Rajabi, G.P. Gibiino, and J. Szatkowski); one in Aveiro, Portugal (D. Ribeiro), and one in Montreal, Canada (K. Wang). These teams competed to perform the most accurate LSNA calibrations possible in their laboratories and then compare those calibrations to a calibration based on the NIST artifacts.

This article describes our joint effort to test this approach for assessing the measurement accuracy of LSNA calibrations. We show that having one trusted reference calibration allows the calibration accuracy of the user's working calibration to be assessed and its performance under a variety of conditions to be inferred. We also demonstrate that the calibration-comparison approach provides additional information that simplifies the identification of sources of error in the user's working calibration.

LSNA Verification Approach

As previously stated, the main objective of the competition was to calibrate a LSNA as accurately as possible (each team was required to use their own calibration standards for this first calibration) and prove that the calibration was accurate by accurately measuring the NIST calibration kit. The NIST calibration kit included a comb generator (Keysight Technologies U9391G) with a 1.85-mm male connector, a two-port electronic calibration unit (Keysight Technologies N4694A) with 1.85-mm male and female connectors, and a traceable power sensor (Rohde and Schwarz NRP-Z57) with a 1.85-mm male connector. The comb generator and electronic calibration unit were precharacterized at NIST, which provided a reference for consistent comparison of the calibrations.

The competitors' calibrations were compared to the NIST calibration according to the procedure described in [10]. The calibrated waves are calculated from the raw measurements by use of the cascade error boxes X and Y . The corresponding schematic is shown in Figure 1. The X and Y error boxes account for the imperfections of the measurement setup and are used to calculate the absolute power and phase of the wave parameters a and b .

For each analyzer port k , we can define approximate bounds Δ_k on the Euclidean norm of differences

in the forward and backward wave parameters a_k and b_k measured with the user's working calibration (cal user) and the traceable calibration (cal NIST) based on the NIST artifacts with

$$\Delta_1 = \frac{\left\| \begin{bmatrix} a_{1,\text{cal user}} - a_{1,\text{cal NIST}} \\ b_{1,\text{cal user}} - b_{1,\text{cal NIST}} \end{bmatrix} \right\|}{\left\| \begin{bmatrix} a_1 \\ b_1 \end{bmatrix} \right\|} \leq \| X_{\text{cal user}} X_{\text{cal NIST}}^{-1} - I \|$$

$$\simeq \| X_{\text{cal NIST}} X_{\text{cal user}}^{-1} - I \| \quad (1)$$

$$\Delta_2 = \frac{\left\| \begin{bmatrix} a_{2,\text{cal user}} - a_{2,\text{cal NIST}} \\ b_{2,\text{cal user}} - b_{2,\text{cal NIST}} \end{bmatrix} \right\|}{\left\| \begin{bmatrix} a_2 \\ b_2 \end{bmatrix} \right\|} \leq \| Y_{\text{cal user}} Y_{\text{cal NIST}}^{-1} - I \|$$

$$\simeq \| Y_{\text{cal NIST}} Y_{\text{cal user}}^{-1} - I \| \quad (2)$$

where a_k and b_k are the incident and scattered waves at the analyzer's port k . Since the exact values of the wave quantities are unknown, it is more convenient to use the approximate bounds of Δ_k , which can be calculated by comparing the error boxes X and Y . The bounds correspond to the upper limit of the sum of the square errors for a given reference calibration at a single frequency point.

The figure of merit (FoM) used in the competition to determine the competition's winner was

$$\text{FoM} = \frac{1}{N} \sum_{n=1}^N \frac{\Delta_1 + \Delta_2}{f_n} \quad (3)$$

where the approximate error bounds are summed and normalized over all the N frequencies f . The frequency term in the denominator was deliberately added to the FoM to encourage contestants to test the procedure to the highest frequency possible in their laboratory. The frequency step was arbitrarily set to 200 MHz. In the ideal case of two equal calibrations, the FoM will be equal to zero. Any deviation from the NIST measurements will result in an increase of the FoM. The competitor with the lowest FoM was declared the winner.

Calibration Procedure

In order to complete the calibration-comparison process, a first-tier user's working calibration (cal user) had to be performed by the contestant. An example measurement system, set up by the Leuven/Warsaw team, is shown in Figure 2. Its schematic, including the order of calibration and measurement steps, is depicted in Figure 3. The heart of the system was the LSNA PNA-X network analyzer from Keysight Technologies, which was required in order to control the states of the electronic calibration unit. The Leuven/Warsaw and Montreal teams used 67-GHz N5247A PNA-Xs, while the Aveiro team used a 50-GHz N5245A PNA-X.

The teams competed to perform the most accurate LSNA calibrations possible in their laboratory and then compare those calibrations to a calibration based on the NIST artifacts.

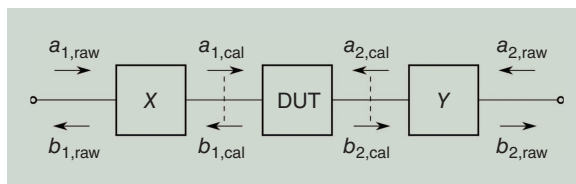


Figure 1. The measurement model for the LSNA with no coupling between ports. Error boxes X and Y are determined in the calibration-comparison procedure. Calibration planes are marked with dashed lines.

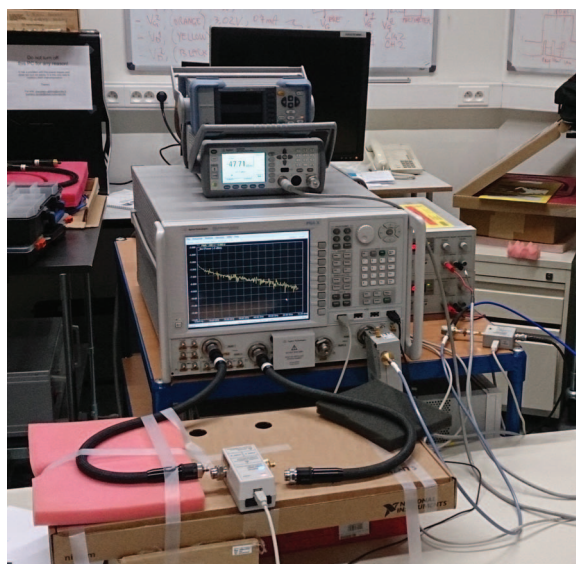


Figure 2. A photo of the measurement system setup used by the Leuven/Warsaw team.

While setting up the system, various precautions were taken by competing teams to ensure accuracy. The Leuven/Warsaw team performed the following steps. In order to minimize temperature drift, all instruments, including the calibration standards, were turned on one day before the actual measurements. Moreover, the room temperature was stabilized to +20 °C. In order to ensure good electrical contact and repeatability of the contacts, all the connectors were cleaned with sharpened toothpicks before making contact. The connectors were tightened to the appropriate torque.

Much attention was paid to the placement of the cables in order to avoid creating tension in the cables. This was achieved by stacking piles of paper under the connected devices until the levels of the corresponding connectors were equal.

This work sets the stage for the expanded use of the calibration-comparison approach as a tool for verifying the accuracy of large-signal vector-network-analyzer measurements.

Phase-stable cables were employed to minimize the phase offset introduced by cable movements. To further diminish the phase shifts, each cable was supported on sponges, and was attached to the table with adhesive tape. During all measurements, the cable attached to port one was kept fixed; only the cable at port two was moved. Minimizing the number of cable movements determined the order of measurements. Intermediate frequency bandwidth during all measurements was set to 5 Hz to reduce the network analyzer noise floor because the output power of the highest harmonic from the comb generator can go as low as -70 dBm.

The team first performed a calibration with one-port standards. Since the comb generator of the setup in Leuven has a female connector, a previously characterized adapter was attached to it permanently. The S -parameters of the adapter were included in the calibration. As the comb generator had to generate an extremely rich spectrum with spectral components every 200 MHz up to 67 GHz, ten averages were used for the calibration in Leuven. Next, the absolute power calibration step was performed with the default signal power at -5 dBm, which is a compromise between the receiver linearity and the uncertainty of the measurements performed with the power sensor.

The Aveiro team also had problems with connector types. Since they were using a 50-GHz system, all of the Aveiro calibration standards had 2.4-mm connectors. Even though 1.85-mm and 2.4-mm connectors can mate with each other, the change in connector sizes creates a sizable discontinuity at the interface. The Aveiro team attempted to remove the impact of this transition by using an adapter-removal calibration and measurement scheme. However, no noticeable improvement was achieved when comparing the direct results with the results employing the transition removal. A better approach may be obtained by developing a model of the 2.4–1.85 mm transition with an electromagnetic simulator. Nevertheless, the repeatability of the connection may still strongly impact the transition response and prevent improved results.

After calibration with one-port standards, the two-port linear part of the calibration was performed. As the PNA-X receivers show best linearity for power levels below -20 dBm at the receiver plane, the power for all linear measurements was set to -10 dBm at the source plane. Several types of calibrations (electronic-calibration-unit/mechanical, unknown/flush-thru) were compared by the Leuven/Warsaw team, and they obtained the best results with a SOLT (i.e., short, open, load, and thru) calibration using a Leuven electronic calibration unit and flush-thru. The calibration began with a flush-thru connection, which allowed the Leuven/Warsaw team to minimize total cable movement. Afterward, the electronic calibration unit was connected. Because this requires substantial cable movement, the cables were allowed to relax and release tension for one full minute before the measurements of the electronic calibration unit were performed.

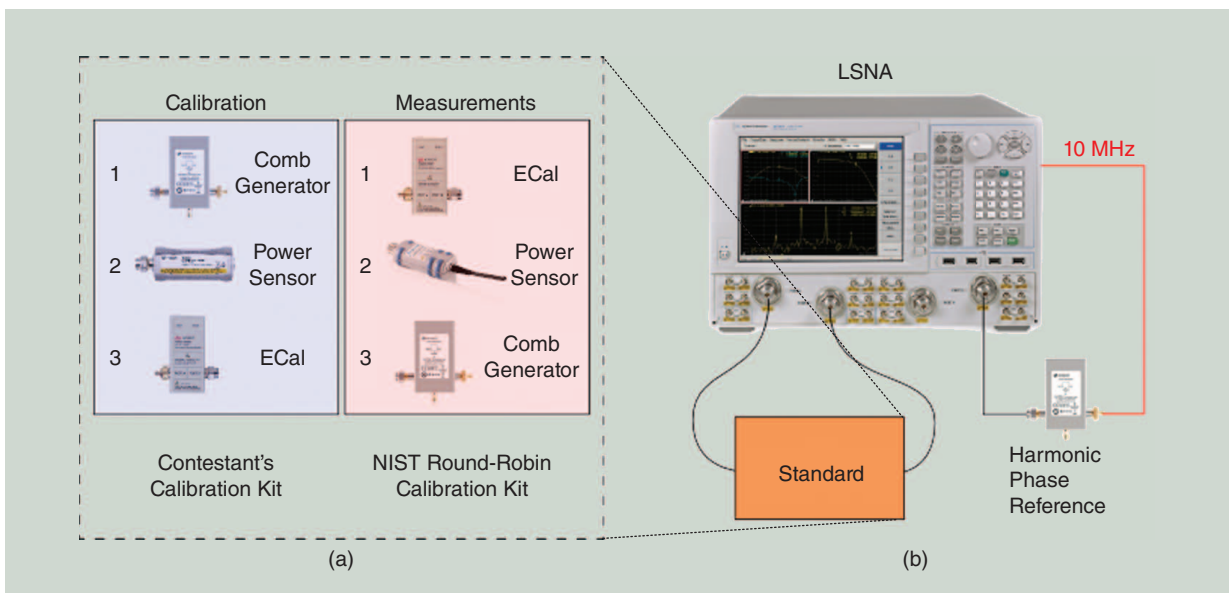


Figure 3. (a) The order of the calibration and measurement steps and (b) the schematic of the measurement setup.

Measurement Procedure

After calibration of the LSNA, measurements of the round-robin calibration kit were performed, using the setup shown in Figure 3. First, the NIST electronic calibration unit was characterized. Because its width is very similar to the electronic calibration unit in user's calibration kit, only a minimal movement of the cable attached to port two was required. Wave quantities were captured for all the states and saved in the .w2p file created by NIST PNA Grabber [11]. The states of the round-robin electronic calibration unit were changed through an interface included in the NIST PNA Grabber.

Then, one-port devices from the round-robin kit were measured, which allowed release of the cable attached to the second port. First, NIST's comb generator was characterized with the same settings as during the calibration. During measurements of the comb signal, the internal generators of the PNA-X were turned off; thus, the phase normalization was also turned off. The reflection coefficient of the comb generator was measured with the clock signal disconnected from the input of the generator, which was terminated with a broadband matched load.

The measurements of the power sensor supplied by NIST were the most cumbersome for all of the groups, as the power had to be captured separately at each frequency. This required proper triggering of the power meter during the sweep. The Aveiro team prepared a LabVIEW procedure, in which the measurements were triggered with an external power supply acting as a trigger source. The time between setting the frequency on the PNA-X and power readout was set to 1 s. The Leuven/Warsaw and Montreal teams used the external instrument control capability available in the PNA-X. While employing such control methods, contestants needed to assure that the correction coefficients stored in the power sensor were applied to the measurement results.

Another problem occurred with instrument power settling. Even though users can enable power measurements only after the power level settles, the power changes turned out to be too abrupt when the internal generators of the PNA-X were switched between certain frequency points. Therefore, automated level control had to be turned on in order to avoid erroneous power readings. Throughout the experiments, each team helped the other teams to complete their measurements by providing software and advice.

Results and Discussion

All the data were analyzed with the NIST Microwave Uncertainty Framework [11], [12]. The results are shown in Figure 4. The corresponding FoM are summarized in Table 1. The results from Leuven/Warsaw and Aveiro teams are similar, while there is something fundamentally wrong with the Montreal mea-

The main objective of the competition was to calibrate a LSNA as accurately as possible.

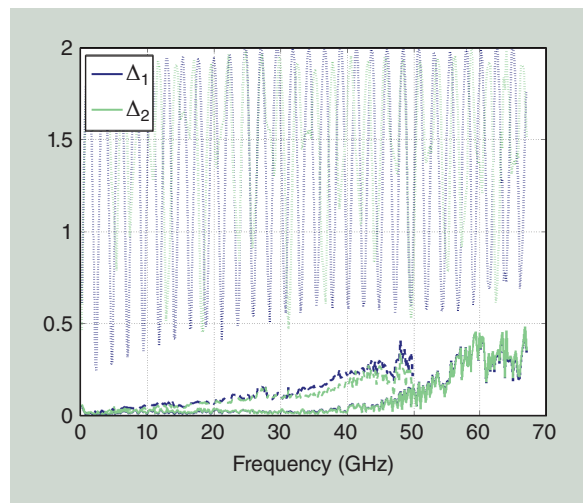


Figure 4. The measurements of Δ_1 and Δ_2 obtained by the competing groups as a function of frequency. Solid lines: results from the Leuven/Warsaw team (up to 67 GHz); dashed lines: results from Aveiro team (up to 50 GHz); dotted lines: results from Montreal team (up to 67 GHz).

surements. After investigation, it was determined that the Montreal team had turned off their first-tier working calibration during the measurements of the NIST artifacts.

The frequency dependence of the Leuven/Warsaw and the Aveiro results were quite different. For the Leuven/Warsaw team, the approximate error boundaries do not exceed 0.05 for frequencies below 40 GHz, while they rapidly rise to as high as 0.45 above 40 GHz. At the same time, the Aveiro results show a constant increase of the approximate error boundaries through the whole frequency range.

To better understand the sources of these discrepancies, the phase and amplitudes of the user and NIST calibrations were set equally, leaving only the errors from the linear vector calibration. The corresponding results following this adjustment are shown in Figure 5. We see that the phase and amplitude adjustments do not significantly improve the FoM for the Aveiro team. Thus, the main source of discrepancy lies in the linear vector calibration. One of the possible causes of

TABLE 1. The FoM calculated from the measurement results obtained by the three competing teams.

| Team | Leuven/ Warsaw | Aveiro | Montreal |
|------|-------------------|----------|----------|
| FoM | 0.007284 | 0.012071 | 0.24556 |

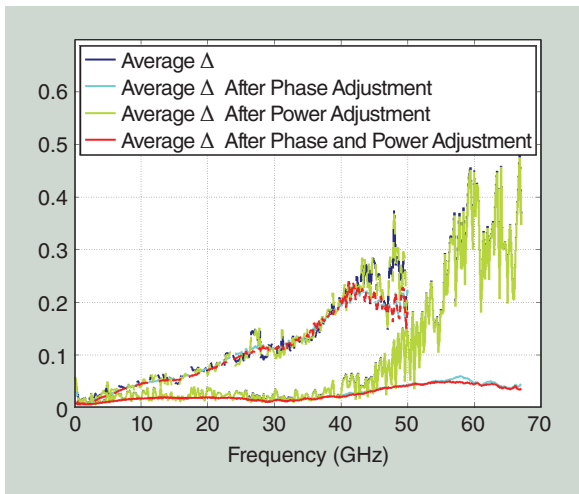


Figure 5. The values of Δ_1 and Δ_2 after phase and power adjustments to the NIST reference results for the Leuven/Warsaw team (solid lines, up to 67 GHz) and the Aveiro team (dashed lines, up to 50 GHz).

this may be the transition between the 2.45-mm and 1.85-mm connectors.

This procedure demonstrated that the discrepancy obtained by the Leuven/Warsaw team was clearly related to the phase difference of the calibrations. This might have been caused by several phenomena. First, the discrepancy can be due to the errors in the characterization of the adapter, which was connected to the comb generator during the first-tier calibration step. It could also have been caused by the lower dynamic range in the measurements at higher frequencies due to the decrement of the comb generator's output power at each tone of the comb signal with increasing frequency. Finally, there might have been differences in the phase calibrations of the NIST and Leuven/Warsaw comb generators.

Based on these results and the FoM as calculated in Table 1, the competition judges awarded the US\$1,250 first-place prize to the Leuven/Warsaw team, the US\$750 second-place prize to the Aveiro team, and the third-place prize—a Keysight EEsof ADS license—to the Montreal team.

Conclusions

This article, as well as the competition, demonstrated the use of the calibration-comparison approach to assessing the accuracy of LSNA calibrations. Easy-to-calculate approximate error bounds were used as the FoM for calibration comparison. By adjusting different calibration components to the reference calibration results, participants were able to identify the sources of error in the competitors' calibrations. This work sets the stage for the expanded use of the calibration-comparison approach as a tool for verifying

the accuracy of large-signal vector-network-analyzer measurements.

Acknowledgments

The Leuven/Warsaw team was supported by the Research Foundation of Flanders (FWO-Vlaanderen) and the Hercules Foundation. P. Barmuta was supported by an IEEE Microwave Theory and Techniques Society Graduate Fellowship and by the European-Union European Social Fund through the Warsaw University of Technology Development Program. A. Lewandowski was supported by the Polish National Science Center under project no. 2011/03/D/ST7/01731. D. Ribeiro was supported by the Fundação para a Ciência e Tecnologia (F.C.T.) under Ph.D. grant SFRH/BD/85163/2012.

Note: The National Institute of Standards and Technology does not endorse commercial products. We mention brand names only to better describe our experiments. Other products may work as well or better.

References

- [1] W. Van Moer and Y. Rolain, "A large-signal network analyzer: Why is it needed?" *IEEE Microwave Mag.*, vol. 7, no. 6, pp. 46–62, 2006.
- [2] A. Rumiantsev and N. Ridler, "VNA calibration," *IEEE Microwave Mag.*, vol. 9, no. 3, pp. 86–99, June 2008.
- [3] D. Humphreys, M. Harper, J. Miall, and D. Schreurs, "Characterization and behavior of comb phase-standards," in *Proc. European Microwave Conf.*, Oct. 10–13, 2011, pp. 926–929.
- [4] H. Reader, D. Williams, P. Hale, and T. Clement, "Comb-generator characterization," *IEEE Trans. Microwave Theory Tech.*, vol. 56, no. 2, pp. 515–521, Feb. 2008.
- [5] J. A. Jargon, D. C. DeGroot, and D. F. Vecchia, "Repeatability study of commercial harmonic phase standards measured by a nonlinear vector network analyzer," in *Proc. Microwave Measurements Conf.*, Dec. 4–5, 2003, pp. 243–258.
- [6] H. Jang, Y. Ko, and P. Roblin, "Development of multiharmonic verification artifact for the LSNA and NVNA (MTT-11)," *IEEE Microwave Mag.*, vol. 14, no. 1, pp. 134–139, Jan.–Feb. 2013.
- [7] S. Adhikari, A. Ghiotto, K. Wang, and K. Wu, "Development of a Large-Signal-Network-Analyzer round-robin artifact," *IEEE Microwave Mag.*, vol. 14, no. 1, pp. 140–145, Jan.–Feb. 2013.
- [8] M. Rajabi, D. A. Humphreys, T. Nielsen, P. Barmuta, and D. Schreurs, "Design and analysis of a verification device for the nonlinear vector network analyzer," in *Proc. Microwave Measurement Conf.*, May 22, 2015, pp. 1–4.
- [9] G. Pailloncy and M. V. Bossche, "Gaining advanced insight in the phase stability of comb generators using a large-signal network analyzer," in *Proc. IEEE/MTT-S Int. Microwave Symp.*, June 3–8, 2007, pp. 1193–1196.
- [10] D. F. Williams, K. A. Remley, J. M. Gering, G. S. Lyons, C. Lineberry, and G. S. Aivazian, "Comparison of Large-Signal-Network-Analyzer calibrations," *IEEE Microwave Wireless Compon. Lett.*, vol. 20, no. 2, pp. 118–120, Feb. 2010.
- [11] National Institute of Standards and Technology. *NIST Microwave Uncertainty Framework*. 2003. [Online]. Available: <http://www.nist.gov/ctl/rf-technology/related-software.cfm>
- [12] J. A. Jargon, D. F. Williams, T. M. Wallis, D. X. Le Golvan, and P. D. Hale, "Establishing traceability of an electronic calibration unit using the NIST Microwave Uncertainty Framework," in *Proc. Microwave Measurement Conf.*, June 22–22, 2012, pp. 1–5.

